ELSEVIER

Materials Science and Engineering B81 (2001) 116–120

MATERIALS SCIENCE & ENGINEERING B

www.elsevier.com/locate/mseb

Spectroscopic studies of the visible and infrared luminescence from Er doped GaN

U. Hömmerich [a,*], J.T. Seo [a], C.R. Abernathy [b], A.J. Steckl [c], J.M. Zavada [d]

[a] *Department of Physics, Research Center Optical Physics, Hampton University, Hampton, VA 23668, USA*
[b] *Department of Materials Science and Engineering, University of Florida, Gainesville, FL 32611, USA*
[c] *Nanoelectronics Laboratory, University of Cincinnati, Cincinnati, OH 45221, USA*
[d] *US Army European Research Office, London, NW 1 5 TH, UK*

Abstract

The visible and infrared luminescence of erbium doped gallium nitride prepared by metal-organic molecular beam epitaxy (MOMBE) and solid-source molecular beam epitaxy (SSMBE) were investigated as a function of excitation wavelength and temperature. Both samples exhibited 1.54 μm Er^{3+} photoluminescence (PL), but only GaN:Er (SSMBE) showed visible PL lines at 537 and 558 nm. Excitation wavelength dependent PL measurements revealed the existence of multiple Er sites leading to an inhomogeneous line broadening of the Er^{3+} intra-4f PL under above-gap pumping. A significant narrowing of the green Er^{3+} PL lines was observed when pumping resonantly into an intra-4f transition. This observation suggests that a specific class of Er^{3+} ions was selectively excited. A temperature dependent study of the PL intensity ratio and lifetime of the green Er^{3+} lines revealed that the two excited states $^2H_{11/2}$ and $^4S_{3/2}$ are thermally coupled. Considering this thermal coupling and assuming that non-radiative decay is negligibly small at low temperatures, the green luminescence efficiency at room temperature was estimated to be near unity.

Keywords: Erbium; Gallium nitride; Visible and infrared luminescence

1. Introduction

The recent demonstration of visible (blue, green, red) and infrared (1.54 μm) electroluminescence from rare earth (RE) doped GaN has spurred significant interest in this class of materials for possible applications in optical communications and full color displays [1,2]. Compared with previously studies semiconductors such as GaAs or Si [3], GaN has some major advantages as a host for Er and other RE dopants. GaN is a wide-gap semiconductor, which leads to a reduced RE emission quenching and the observation of strong RE emission at room temperature. In addition, initial studies have shown that RE ions can be incorporated into GaN at concentrations as high as at least 1×10^{21} cm^{-3} [1,2]. In order to optimize the performance of current RE doped GaN devices it is important to obtain a better understanding of the RE incorporation, excitation schemes, and luminescence efficiency. In this paper, we present new spectroscopic results of the photoluminescence (PL) properties of Er doped GaN and discuss them in terms of different Er centers and Er luminescence efficiency.

2. Experimental details

The Er doped GaN sample prepared by metalorganic molecular beam epitaxy (MOMBE) was grown in an INTEVAC Gas Source Gen II on In-mounted (100) Si substrate [4]. The GaN film was preceded by a low temperature AlN buffer ($T_g = 425$°C). An undoped GaN spacer 0.2 μm thick was deposited prior to the growth of GaN:Er. Triethylgallium (TEGa) and dimethylethylamine alane (DMEAA) provided the group III fluxes. A shuttered effusion oven with 4N Er was used for solid source doping. Reactive nitrogen species were provided by a SVT radio frequency (rf) plasma source. The Er concentration in the sample was $\sim 8 \times 10^{18}$ cm^{-3}. Due to the incorporation of carbon

* Corresponding author. Tel.: +1-757-7275829; fax: +1-757-7286910.
E-mail address: uwe.hommerich@hamptonu.edu (U. Hömmerich).

0921-5107/01/$ - see front matter
PII: S0921-5107(00)00680-2

and oxygen from residual ether in TEGa, the C and O background were $\sim 10^{21}$ and $\sim 10^{20}$ cm^{-3}, respectively, as measured by SIMS.

The Er doped GaN sample prepared by solid-source molecular beam epitaxy (SSMBE) was grown in a Riber MBE-32 system on Si (111) substrates [5]. Ga and Er solid sources were used in conjunction with a RF plasma source supplying atomic nitrogen. The sample was pretreated by cleaning in acetone, methanol, and deionized water before insertion into the loadlock. The sample was subsequently outgassed at ~ 950°C before growth. During the growth, the Ga cell temperature was kept constant for a beam equivalent pressure of $\sim 8.2 \times 10^{-7}$ Torr. The RF-plasma source was kept constant at 400 W with a N_2 flow rate of 1.5 sccm, corresponding to a chamber pressure of mid -10^{-5} Torr. The growth temperature was varied from 750 to 950°C and the Er cell temperature was maintained at 1100°C. The Er concentration in the sample was determined to be $\sim 2 \times 10^{20}$ cm^{-3}.

Photoluminescence spectra were measured using either the UV argon laser lines (333.6–363.8 nm) or a visible argon laser line at 496.5 nm. Infrared PL spectra were recorded using a 1-m monochromator equipped with a liquid-nitrogen cooled Ge detector. In visible PL studies a thermo-electric cooled photomultiplier tube was employed for detection. The signal was processed using lock-in techniques. The obtained PL spectra were not corrected for the spectral response of the setup. Visible lifetime data were taken by resonantly pumping into the $^2H_{11/2}$ Er^{3+} transition at ~ 537 nm using an Optical Parametric Oscillator system (10 Hz, 5–10 ns pulses). A digitizing oscilloscope was employed for processing the lifetime transients.

3. Results and discussion

An overview of the normalized visible and infrared luminescence from Er doped GaN prepared by MOMBE and SSMBE is shown in Fig. 1. The PL was excited using the multi-line UV (333.6–363.8 nm) output of an argon ion laser, which corresponds to above-gap pumping. Both samples exhibited weak bandage luminescence (not shown) [6], a defect-related background PL band peaking around 550 nm, and a narrow-band intra-4f Er^{3+} luminescence at 1.54 μm arising from the $^4I_{13/2} \rightarrow {}^4I_{15/2}$ transition. In addition, GaN:Er (SSMBE) also showed intra-4f Er^{3+} luminescence located at 537 nm ($^2H_{11/2} \rightarrow {}^4I_{15/2}$), 558 nm ($^4S_{3/2} \rightarrow {}^4I_{15/2}$), 667 nm ($^4F_{9/2} \rightarrow {}^4I_{15/2}$), and 1000 nm ($^4I_{11/2} \rightarrow {}^4I_{15/2}$). It is somewhat surprising that these Er lines were not observed in the GaN:Er (MOMBE) sample, even thus this sample showed a weaker background PL compared with the GaN:Er (SSMBE) sample.

High resolution spectra of the 1.54 μm infrared luminescence are shown in Fig. 2. At room temperature the width (FWHM) of the central emission line was estimated to be ~ 12 nm for GaN:Er (MOMBE) and ~ 9 nm for GaN:Er (SSMBE). At 15 K, the PL spectra narrowed significantly and some sharp structure was observable from GaN:Er (SSMBE). The low temperature linewidth was determined to be ~ 5 nm for GaN:Er (MOMBE) and ~ 1.5 nm for GaN:Er (SSMBE), respectively. These linewidths are orders of

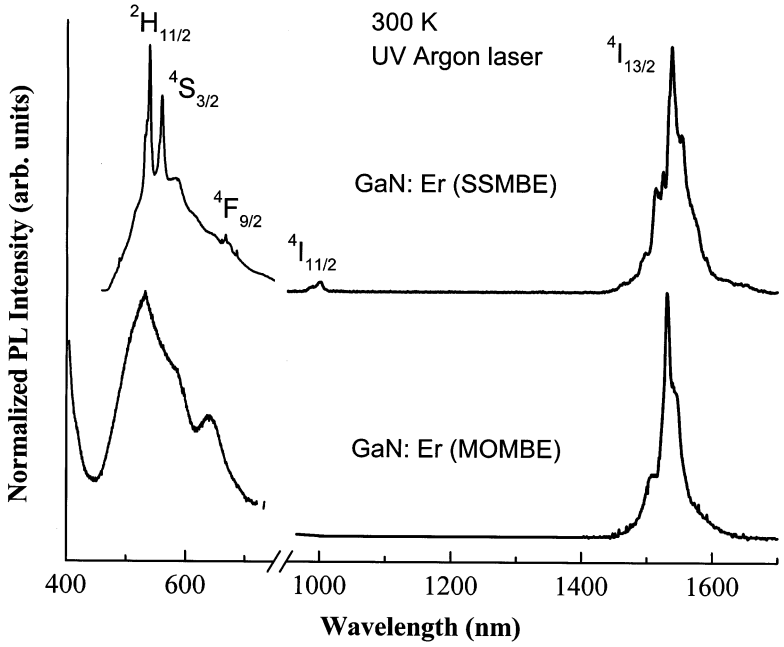

Fig. 1. Overview of the visible and infrared luminescence from Er doped GaN prepared by MOMBE and SSMBE.

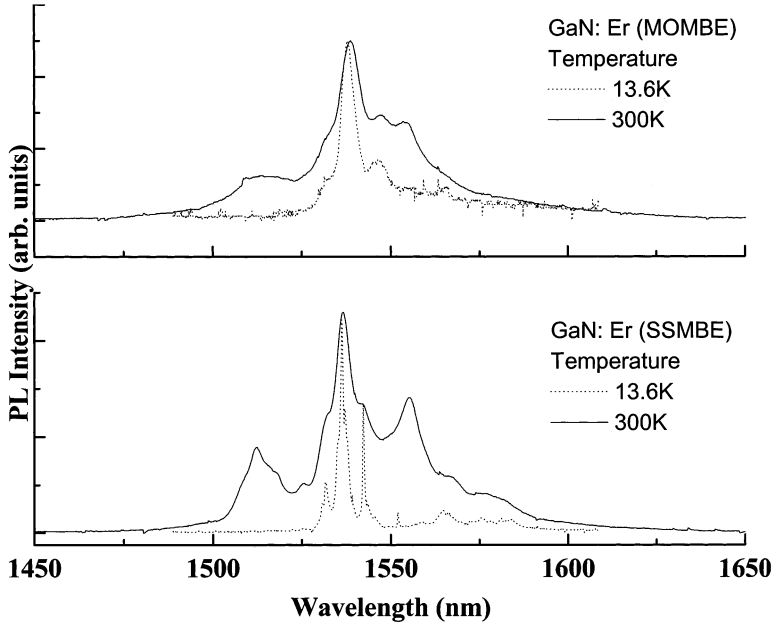

Fig. 2. High resolution 1.54 μm PL spectra at 15 K (dotted line) and 300 K (solid line).

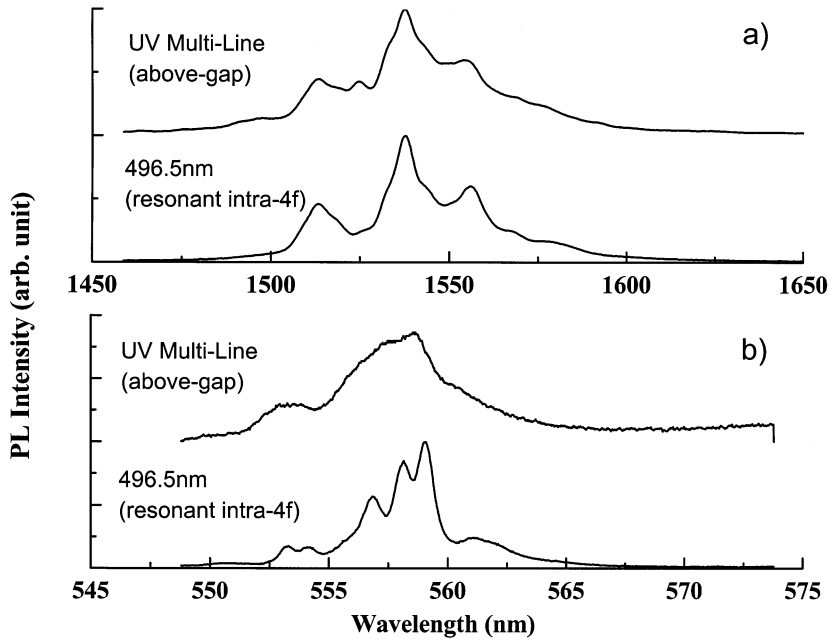

Fig. 3. Room temperature PL spectra for different excitation wavelengths, (a) infrared; (b) visible.

magnitude larger than those reported for Er doped GaAs ($< \sim 0.03$ nm at 2 K) [7], which is most likely due to a combination of Stark splittings in the $^4I_{13/2}$ and $^4I_{15/2}$ states and inhomogeneous broadening arising from Er^{3+} ions located in slightly different local environments.

The existence of multiple Er sites in GaN prepared by SSMBE is supported by an excitation wavelength dependent study of the Er^{3+} PL spectra. It can be noticed in Fig. 3a, that pumping resonantly into an intra-4f transition ($\lambda_{ex} = 496.5$ nm) leads to a slightly reduced linewidth of the central 1.54 μm emission peak (~ 8 nm) compared with above-gap pumping. This effect was even more pronounced for the visible emission line at ~ 558 nm shown in Fig. 3b. Some fine structure was clearly resolved under resonant pumping with individual lines having a width ~ 1.4 nm. Under above-gap excitation only a broad line with a width of ~ 4.3 nm was observed. These results suggest that only a subset of Er^{3+} ions are excited when pumping reso-

nantly into an Er^{3+} level. Moreover, it was also noticed that the visible PL lifetime was nearly single-exponential under resonant excitation compared with a non-exponential decay time observed under above-gap excitation. A more detailed study on the spectroscopy of the different Er^{3+} sites in GaN:Er (SSMBE) is in progress.

More information on the green luminescence lines was drawn from temperature dependent PL studies pumping resonantly at either 496.5 nm ($^4I_{15/2} \rightarrow {}^4F_{7/2}$) or 537 nm ($^4I_{15/2} \rightarrow {}^2H_{11/2}$). The temperature dependence of the lifetime monitored at 558 nm (λ_{mon}) and excited at 537 nm (λ_{ex}) is shown in Fig. 4. At 15 K the lifetime was determined to be 11.2 μs which reduced to 6.2 μs at room temperature. The shortening in the lifetime with increasing temperature can be caused by a number of different processes including a temperature dependent radiative decay rate, non-radiative decay through multiphonon relaxation or energy transfer. Several authors have reported the thermalization of the $^4S_{3/2}$ and $^2H_{11/2}$ states for Er doped insulators [8]. The thermal coupling leads to a common decay time τ, which can be described as:

$$\frac{1}{\tau} = \frac{\tau_s^{-1} + \tau_H^{-1} g_H/g_S \exp(-\Delta E/kT)}{1 + g_H/g_S \exp(-\Delta E/kT)} \quad (1)$$

where τ_H and τ_S are the intrinsic radiative decay times of the $^2H_{11/2} \rightarrow {}^4I_{15/2}$ and $^4S_{3/2} \rightarrow {}^4I_{15/2}$ transitions, respectively, g_H and g_S are their electronic degeneracies ($2J+1$), and ΔE is the energy difference between both exited states ($\Delta E = 87$ meV).

At low temperature the $^2H_{11/2}$ state is not thermally populated and no luminescence is observed at 537 nm (Fig. 5a). Assuming that non-radiative processes are negligibly small, the lifetime measured at 15 K is interpreted as the intrinsic decay time of the $^4S_{3/2} \rightarrow {}^4I_{15/2}$ transition, i.e. $\tau_S = 11.2$ μs. The intrinsic lifetime of the $^2H_{11/2} \rightarrow {}^4I_{15/2}$ was determined indirectly from the temperature dependence of the luminescence intensity of the green Er^{3+} lines at 537 and 558 nm shown in Fig. 5b. Considering the thermal coupling of the involved states, the intensity ratio of both lines was fitted to an expression:

$$I_H = \frac{\tau_S g_H h w_H}{\tau_H g_S h\omega_S} \exp\left(-\frac{\Delta E}{kT}\right) \quad (2)$$

with $h\omega_H = 2.31$ eV, $h\omega_S = 2.22$ eV, $\tau_S = 11.2$ μs, and $\Delta E = 87$ meV. The intrinsic lifetime of the $^2H_{11/2} \rightarrow {}^4I_{15/2}$ transition was taken as a fitting parameter and a value of $\tau_H \sim 0.92$ μs was obtained. Using this set of parameters the temperature dependence of the luminescence lifetime was calculated using Eq. (1) as shown in Fig. 4b (solid line). A good agreement between experimental data and theory was achieved using a consistent set of parameters. This modeling indicates that the decrease of the luminescence lifetime with temperature is mainly due to an increased radiative decay rate arising from the fast thermalization of the $^2H_{11/2} \rightarrow {}^4I_{15/2}$ and $^4S_{3/2} \rightarrow {}^4I_{15/2}$ transitions. This preliminary analysis of the lifetime implies that non-radiative decay processes are small and, therefore, the green luminescence efficiency is near unity.

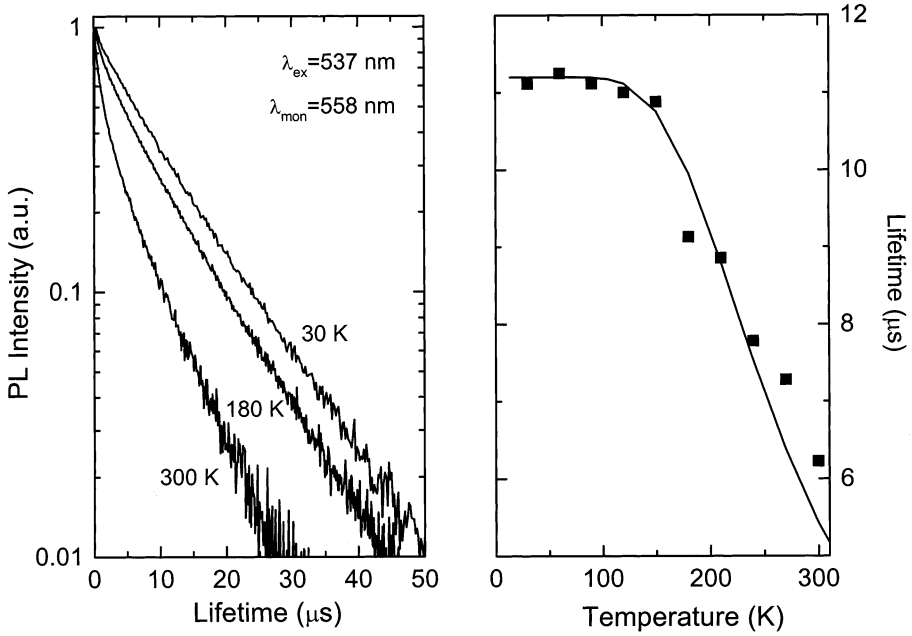

Fig. 4. (a) Luminescence lifetime curves at 30, 180, and 300 K. (b) Temperature dependence of the luminescence lifetime from 15 to 300 K.

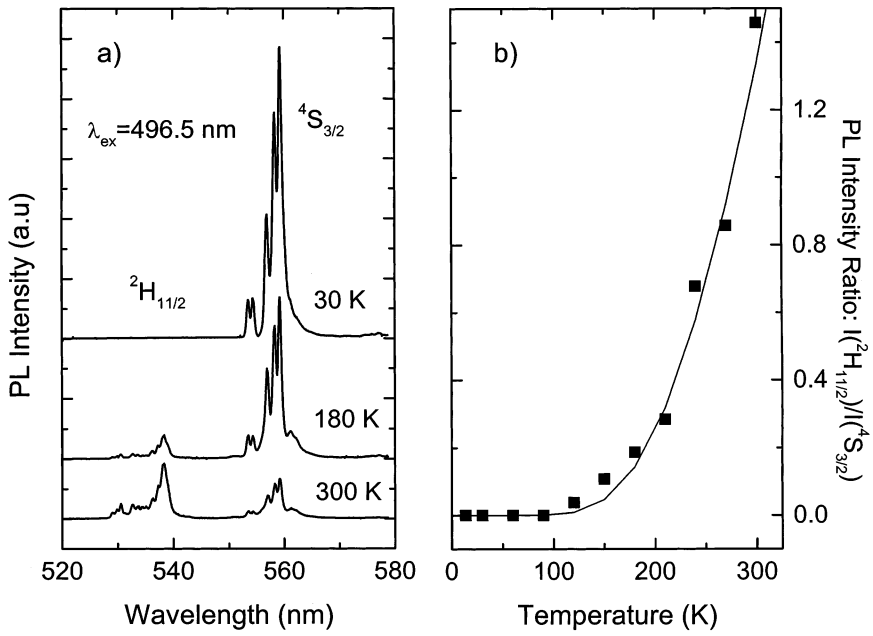

Fig. 5. (a) Temperature dependence of the green luminescence lines at 15, 180, and 300 K. (b) Integrated PL intensity ratio of the green PL lines.

4. Conclusions

The infrared and visible luminescence properties of Er doped GaN prepared by MOMBE and SSMBE were studied as a function of temperature and excitation wavelength. Under above gap excitation, both samples exhibited characteristic 1.54 μm PL arising from the $^4I_{13/2} \rightarrow {}^4I_{15/2}$ intra-4f Er^{3+} transition. The room temperature linewidths of the central emission peak were determined to be $\sim$12 nm for GaN:Er (MOMBE) and $\sim$9 nm for GaN:Er (SSMBE), respectively. Based on excitation wavelength dependent PL and lifetime measurements it was concluded that the relatively large linewidths are partially due to multiple Er sites in the samples. The exact nature of these Er sites is not yet fully understood and needs further investigation. Besides 1.54 μm PL, GaN:Er (SSMBE) also emitted intense green PL at $\sim$537 and $\sim$558 nm. Compared with above-gap excitation, the visible lines narrowed significantly under resonant pumping into an intra-4f Er^{3+} transition. This observation suggests a selective excitation of a subset of Er^{3+} ions. The temperature dependence of the green PL lifetime and intensity ratio reflects the thermalization of the $^2H_{11/2}$ and $^4S_{3/2}$ excited states. Considering this thermal coupling, the efficiency of the green luminescence under resonant pumping was estimated to be near unity. More investigations of the luminescence efficiency as a function of excitation wavelength and Er concentration are in progress.

Acknowledgements

The authors from Hampton University acknowledge financial support by ARO through grant DAAD19-99-1-0317 and NASA through grant NCC-1-251. The work at University of Florida was supported by ARO grant DAAH04-96-1-0089. The work at University of Cincinnati was supported by ARO grant DAAD19-99-1-0348.

References

[1] A.J. Steckl, J.M. Zavada, MRS Bull. 24 (9) (1999) 33–38.
[2] A.J. Steckl, J. Heikenfeld, M. Garter, R. Birkhahn, D.S. Lee, Compound Semicond. 6 (1) (2000) 48.
[3] Rare Earth Doped Semiconductors II, in: S. Coffa, A. Polman, R.N. Schwartz (Eds.), Materials Research Society Proceedings, vol. 422, 1996.
[4] J.D. MacKenzie, C.R. Abernathy, S.J. Pearton, U. Hömmerich, J.T. Seo, R.G. Wilson, J.M. Zavada, Appl. Phys. Lett. 72 (1998) 2710.
[5] A.J. Steckl, R. Birkhahn, Appl. Phys. Lett. 73 (1998) 1700.
[6] U. Hömmerich, J.T. Seo, J.D. MacKenzie, C.R. Abernathy, R. Birkhahn, A.J. Steckl, J.M. Zavada, MRS Internet J. Nitride Semicond. Res. **5S1**, W11.65 (2000) (http://nsr.mij.mrs.org/5S1/W11.65/)
[7] H. Nakagome, K. Uwai, K. Takahei, Appl. Phys. Lett. 53 (1988) 1726.
[8] M. Shojiya, M. Takahashi, R. Kanno, Y. Kawamoto, K. Kadono, J. Appl. Phys. 82 (1999) 6259.